Novel 1-(4-chlorophenyl)-3-(2-ethoxyphenyl)triazene ligand: Synthesis, X-ray crystallographic studies, spectroscopic characterization and DFT calculations

Fatemeh Valinia [a,*], Nasrin Shojaei [a], Parisa Ojaghloo [a]

[a] Department of Chemistry, Payame Noor University, Tehran, Iran

ARTICLE INFO

ABSTRACT

In the present work, a combined theoretical and experimental investigation on the properties of 1-(4-chlorophenyl)-3-(2-ethoxyphenyl)triazene is reported. The optimized geometry was calculated by B3LYP method using 6-311++G(2d,p) as a large basis set. The FT-IR spectrum was calculated at this level of theory, and was interpreted in terms of potential energy distribution (PED) analysis. The scaled theoretical frequencies were in line with the experimental ones. Furthermore, natural bond orbital (NBO) and atoms in molecules (AIM) theories were used to characterize intra-molecular hydrogen bond. The low value of charge transfer and the absence of bond critical point between O···HN show that there is not intra-molecular hydrogen bond.

1. Introduction

Triazene compound, characterized by having a di-azoamino group (–N=N– N–) commonly adopt a *trans* configuration in the ground state [1]. Triazenes and anionic triazenide [RN=N–NR]⁻ ligands could show different types of coordination modes in metal complexes like monodentate, (N₁,N₃)-chelating towards one metal atom or (N₁,N₃)-bridging over two metal atoms [2].

The first extensive investigation of the coordination chemistry of a triazene derivative (1,3-diphenyltriazene) was carried out in 1887 by Meldola [3] Triazene compounds have been studied for over 130 years concerning their interesting structural, anticancer, and reactivity properties. They have been used in medical, and as organometalic ligands [4].

Triazenes are well known and important substances, especially for synthesis of supramolecular compounds of transition metals like Cu and Hg(II) [5].

The study of transition metal complexes 1,3-diaryl triazenide ligands has increased greatly in the past few years, because of their potential reactivity in relation to their coordination modes [6]. One and double-chained triazenes are well known as important ligands. Besides their ability to coordinate of different manners with transition metals, they are also proficient to assemble unique supramolecular aggregates, because of their remarkable aptitude to attain intermolecular, secondary metal–ligand and ligand–ligand interactions [7].

Literature survey reveals that to the best of our knowledge the synthesis of 1-(4-chlorophenyl)- 3-(2-ethoxyphenyl)triazene (**CET**) has not been reported. Thus, the aim of this study is to synthesize and characterize **CET** and perform DFT computation and analysis. We hereby report our results.

2. Experimental

2.1. General Method

Melting point was determined by Gallenkamp melting point apparatus. Elemental analysis was performed with Perkin-Elmer 2400 series II. ¹H NMR and ¹³C NMR spectra were recorded with Bruker Avance 300 spectrometer with the processing software XWINNMR

* Corresponding author: e-mail: valinia_f@gmail.com

version 3.1.
Chemical shifts are reported on δ scale relative to TMS. FT-IR spectra were measured by a PerkinElmer spectrum RXI FT-IR spectrometer in the frequency range of 4000–400cm^{-1} using KBr discs.

The IR spectrum was recorded at room temperature at the spectral resolution of 1 cm^{-1}. Single crystal X-ray data were collected on a Bruker SMART 1000 CCD area detector (Mo Kα radiation) at 120 K. The crystal was solved by direct methods using SHELXS-97 and refinement was carried out with full-matrix least-squares methods based on F^2 with SHELXL-98 software package [8,10].

   The crystal data and experimental parameters are given in Table 1S (Supplementary information). The parameters in the CIF form are available as Electronic Supplementary Information from the Cambridge Crystallographic Data Centre (CCDC 814968).

2.2. Synthesis

The synthetic route is shown in Scheme 1. A 1000 mL flask was charged with 100 g of ice and 100 mL of water and then cooled to 0 ºC in an ice-bath. After that a solution of containing 6.35 g (0.05 mol) of 4-chloroaniline in 25 mL of methanol and 10 mL (0.12 mol) of hydrochloric acid (d = 1.18 g mL^{-1}) were added to the mixture, and then a solution of NaNO$_2$ containing 3.45 g (0.05 mol) in 25 mL of water was added during 15 min under stirring solution.

   Afterwards, 6.85 g (0.05 mol) of 2-ethoxyaniline was added with vigorous stirring for a period of 30 min to this mixture.
   Finally, to the solution was added sodium acetate 18% until pH: 7-8 was obtained and stirred for 2 hours. The yellow residue was filtered and dissolved in diethyl ether, after evaporation of diethyl ether, a purified orange crystals was obtained, which has a melting point of 56 - 58ºC. Yield: 85%. Infrared and ^{1}HNMR spectra and CHN analysis, were confirmed the **CET** structure.

   ^{1}H NMR (300 MHz, DMSO-d$_6$): δ 1.31 - 1.35 (3H, t, CH$_2$), 4.04 - 4.11 (2H, q, CH$_3$), 6.90 - 7.55 (8H, m, phenyl protons) and 12.66 (1H, s, NH). ^{1}H NMR (300 MHz, Acetone): δ 1.36 - 1.48 (3H, t, CH$_2$), 4.11 - 4.18 (2H, q, CH$_3$), 6.95 - 7.65 (8H, m, phenyl protons) and 10.63 (1H, s, NH). ^{13}C NMR (300 MHz, DMSO-d$_6$): δ 152.82, 148.58, 140.93, 138.90, 130.97, 130.15, 129.30, 128.11, 125.57, 120.59, 116.20, 112.67, 63.76 and 14.79. ^{13}C NMR (300 MHz, CDCl$_3$): δ 148.52, 147.66, 132.77, 131.94, 131.38, 130.02, 129.93, 129.54, 124.75, 121.87, 117.22, 113.14, 65.90 and 16.39.
   IR (KBr, ν cm^{-1}): 3403 (N-H), 3332-2889 (C-H, sp^2), 1595-1514 (C=C), 1487-1294 (C-C), 1453 (N=N), 1156 (N-N), 1041 (ph-Cl).
   Elemental analysis, Found: C, 61.05; H, 4.98; N, 15.18. Calc. for (C$_{14}$H$_{14}$ClN$_3$O): C, 60.98; H, 5.12; N,

15.24 % .
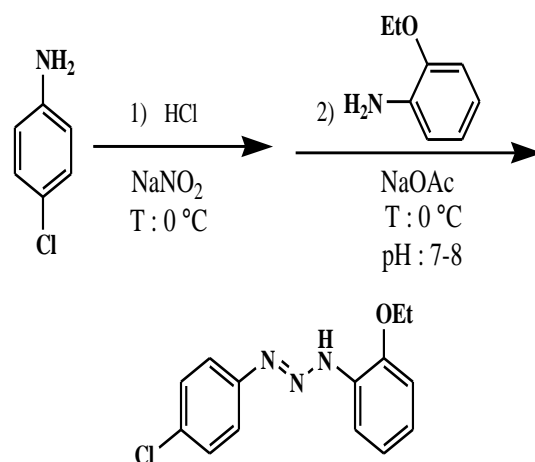
Scheme 1. Synthesis of **CET**

3. Computational details

   Starting geometry for optimization was taken from the X-ray crystallography data. The geometry was then fully optimized at the level of B3LYP/6-311++G (2d,p). The optimization keyword (FOPT) was combined with the frequency calculations (FREQ) to obtain vibrational spectra. In addition, true minimum structure was tested by searching the number of imaginary frequencies (NIMAG). In our output NIMAG was equal to zero, denoting that the optimized structure was not saddle point in the potential energy surface. DFT calculation was done by Gaussian 03 program [11].
   Natural bond orbital calculation was conducted by NBO 3.1 [12] program that has been included in the Gaussian program. Atoms in molecules theory of Bader [13] was studied by the program AIM2000 [14]. The vibrational band assignments were made by using VEDA 4 program [15]. GaussSum [16] was used to calculate group contributions to the molecular orbitals and to prepare the partial density of states (DOS) spectra. All calculations were done by Intel® server SR2600URLX model with 8GB DDR3 of RAM.

4. Results and discussion

4.1. Crystal structure and molecular geometry
   The title compound was purified by recrystallization from diethyl ether. The analytical and spectroscopic data are consistent with the proposed structure. The Ortep diagram of the title compound is given in Fig. 1a. Fig. S1 (Supplementary information) showed the crystal cell of title compound.This compound crystallized in the monoclinic system, space group *P2(1)/n* with four molecules in the unit cell. The unit cell parameters are: *a* = 9.3156(3) Å, *b* = 6.1822(2) Å, *c* = 24.5109(8) Å. The final R value was 0.0449 for 4122 reflections. The title compound, C$_{14}$H$_{14}$ClN$_3$O, is characterized by X-ray analysis and exhibits a *trans* geometry about the N=N double bond in the solid state.

(a)

(b)

(c)
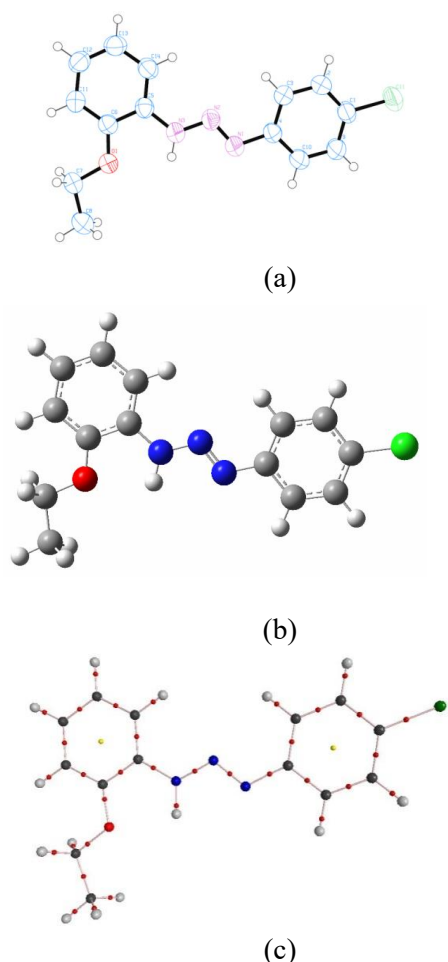
Figure 1. (a) Ortep diagram and (b) optimized theoretical structure of studied molecule at level of B3LYP/6-311++G(2d,p); (c) Molecular graph of the studied molecule at the level of B3LYP/6-311++G(2d,p). Small red sphere, small yellow sphere, and lines represent bond critical points (BCP), ring critical points (RCP), and bond paths, respectively.

The C8–N3–N2–N1 and C9–N1–N2–N3 torsion angles are -177.37° and -178.87°, respectively. A typical feature of free 1,3-diaryltriazenes is delocalization of the π electrons on the triazene group towards to the terminal aryl substituents. This behavior is supported by the deviations observed from the normal N–N and C_{Aryl}–N bond lengths. The N=N bond [1.257 Å] is longer than the characteristic value for a double bond (1.236 Å), whereas the N–N bond [1.325 Å] is shorter than the characteristic value for a single bond (1.404 Å).[17] On the other hand, the N3–C8 [1.395 Å] and N1–C9 [1.422 Å] bonds are shorter than the characteristic N–C_{Aryl} single bonds (secondary amines, R_2NH, R= Csp²; 1.452 Å) [18].

Theoretical and experimental optimized geometry of the title compound is shown in Fig. 1. The experimental and theoretical structural parameters containing bond lengths, bond angles, and dihedral angles are presented in Table 2S. Fig. 2a shows the correlation between theoretical and experimental bond lengths at the level of B3LYP/6-311++G(2d,p).

Fig. 2b shows the correlation for the bond angles. While the correlation coefficient for the bond length is

0.9932, it is only 0.9784 for the bond angles. In other words, the differences between experimental and theoretical bond angles are higher than the differences between experimental and theoretical bond lengths. The reason of these discrepancies is that in the gas phase an individual molecule is considered, while in the solid phase crystal more than one molecule present. Inspecting the experimental structure, it shows that the intermolecular interactions have the most effects on C3-C4-N1, C4-N1-N2, and N2-N3-C5 bond angles. Omitting these values from the graph, the correlation coefficient increases from 0.9784 to 0.992.
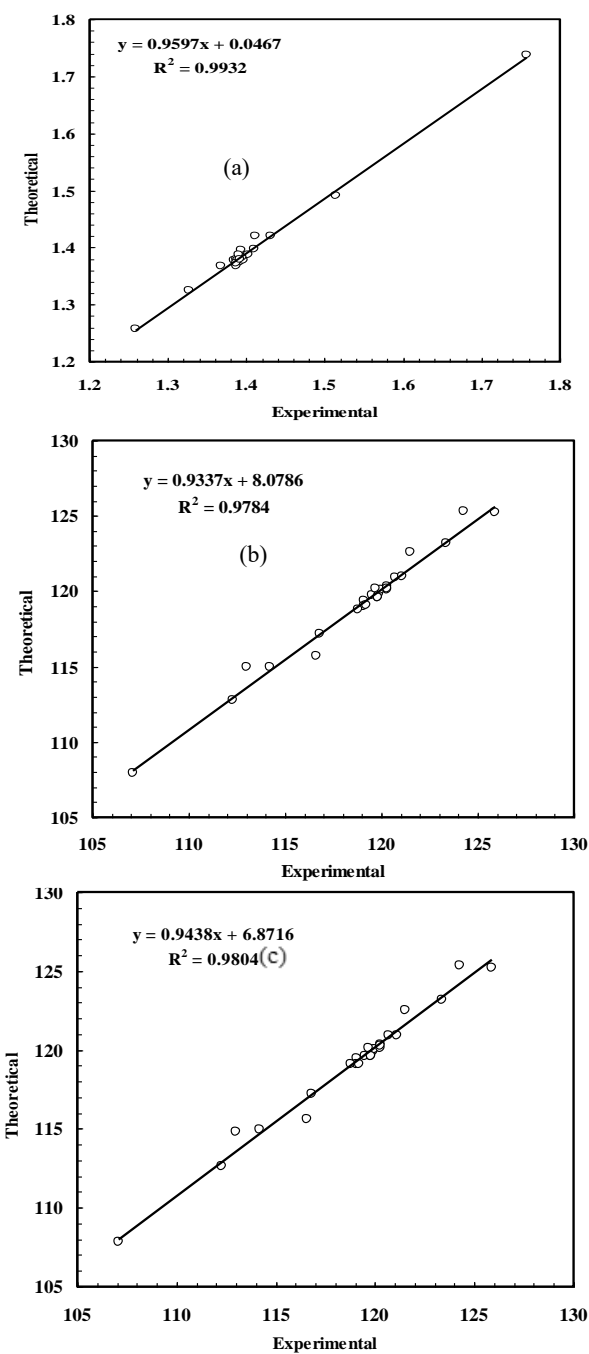
Figure 1. Correlation between theoretical and experimental bond length at the level of B3LYP/6-311++G(2d,p) (a), bond angles at the levels of B3LYP/6-311++G(2d,p) (b) and B3LYP/6-311+G(d) (c).

As noted in above, in the solid phase, contrary to the gas phase, there are inter-molecular interactions between different molecules that they are present in the crystal. With enlarging basis set in the gas phase model, the differences between theory and experiment are increased. This is due to the absence of inter-molecular interactions in the gas phase. Fig. 2c shows the correlation graph for 6-31+G(d) as a small basis set. This basis sets does not change the starting geometry very much. It should be noted that the starting geometry has been taken from the experimental cif file. With this change in basis set, correlation coefficient increases from 0.9784 to 0.9804.

4.2. Vibrational assignment

The title molecule has 33 atoms; therefore, it has 93 normal modes. Experimental and theoretical FT-IR spectra are shown in Fig. 3.

Figure 3. The experimental and calculated (B3LYP/6-311 ++G(2d,p) level) FT-IR spectra of CET; correlation between theoretical and experimental FT-IR spectrum at the level of B3LYP/6-311++G(2d,p) also shown.

The theoretical frequencies and IR intensities were calculated at the level of B3LYP/6-311++G(2d,p). Table 3S shows the detailed vibrational assignment obtained

from the calculated potential energy distribution (PED). Comparing the theoretical frequencies with experimental values reveals that the theoretical frequencies are over-estimated.
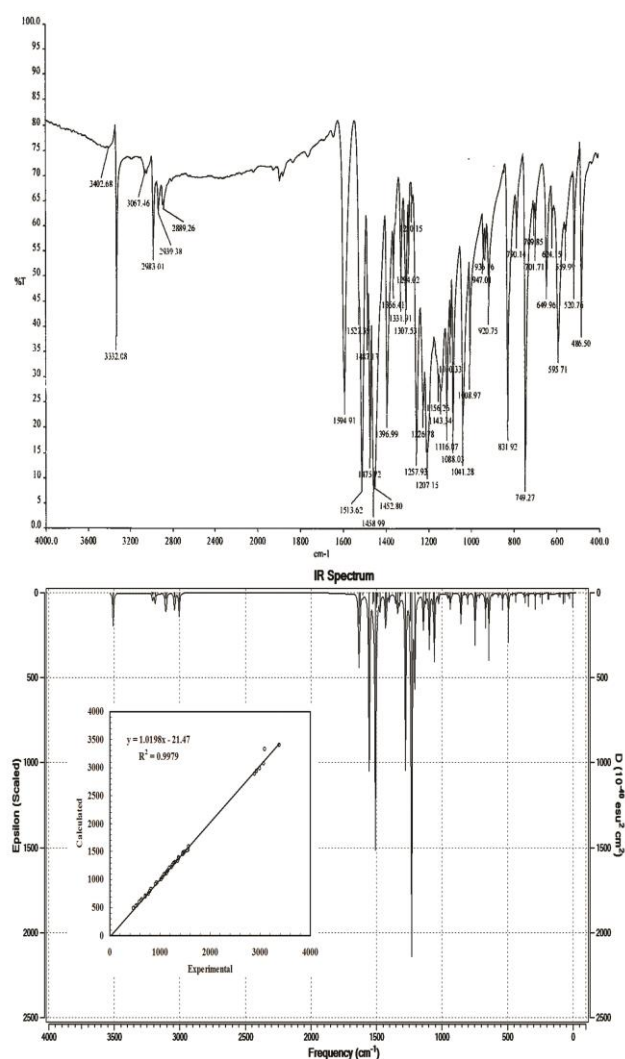
This overestimation is related to the harmonicity in the theoretical models and anharmonicity in real systems. In order to improve the theoretical frequencies to agree with the experiments, a scaling factor is usually used. In this paper, we have used the scaling factor value of 0.9618 that belongs to the 6-311+G(2d,p) basis set.[19] Andersson and Uvdal have shown that the difference between the scaling factor values of + and ++ diffusion functions is only 0.0004 [19].

Therefore, we have used this scaling factor value for our basis set 6-311++G(2d,p). Results of Table 3S show that this scaling factor can represent experimental data in a good way. Fig. 3 shows the correlation between experimental and theoretical vibrational frequencies. The correlation coefficient value of 0.9979 shows that good assignment have been done for the experimental data. In our calculations <EPm> has been increased to the value of 74.76 by using different techniques in the VEDA program. The more <EPm>, the better assignment is.

The aromatic structure shows the presence of C–H stretching vibration in the region 3100–3000cm^{-1}, which is the characteristic region for the ready identification of C–H stretching vibration [20,21].

In this region, the bands are not affected appreciably by the nature of the substituent. The four expected C–H stretching vibrations correspond to stretching modes of C11–H, C12–H, C13–H, C14–H, C2–H, C3–H, C9–H, C10–H units. Therefore in our present work, the FT-IR bands observed at 3332.08, 3067.46, 2983.01, 2939.38 and 2889.26 cm^{-1} are assigned to C–H stretching vibrations. The scaled vibrations by B3LYP/6-311++G(2d,p), method shows very good agreement with recorded spectral data. The aromatic C–H in-plane bending and out-of-plane bending vibrations normally occurs in the region 1300–1000 cm^{-1} and 750-1000 cm^{-1} respectively [22,23], the bands are sharp but have weak-to medium intensity. The C-H in-plane bending vibration computed at 1141.89, 1137.76, 1098.79, 1084.56, 1080.61 and 987.79 by B3LYP method shows excellent agreement with FT-IR bands at 1143.34, 1100.33 and 1088.03cm^{-1} in FT-Raman spectrum. The bands observed at 947.01, 936.16, 831.92 and 790.14 cm^{-1} in FT-IR are assigned to C-H out-of-plane bending vibration for **CET**. This also shows good agreement with theoretically scaled harmonic wavenumber values at 938.86, 932.42, 925.41, 886.01, 823.98, 821.09, 802.73 and 797.26 cm^{-1} by B3LYP method. These C–H in-plane and out-of-plane bending vibrations show good agreement with literature data [24-26] All the C-H vibrational bands are in the expected region and are with almost strong intensity since there is no collision on the benzene structure.

The ring stretching vibrations (C=C) are very much prominent in the spectrum of benzene and its derivatives and are highly characteristic region of the mono substituted aromatic ring itself[27]. The bands between 1520-

1650 cm^{-1} in benzene derivatives usually assigned to C=C stretching modes [28]. The C=C stretching vibrations have been found at 1595, 1527 and 1514 cm^{-1} in this molecule. The assigned values are mostly in expected range whereas the last one is shifted away from the range.

Ring C-C stretching vibrations normally occur in the region 1590-1430 cm^{-1}[29,30]. In the present case, the C-C stretching vibrations have been assigned at 1487, 1397, 1307 and 1294 cm^{-1}. When compared to the literature range cited above, two bands are missing and there is a considerable decrease in frequencies which are due to the strong coupling of N=N between the ring and worsening with the increase of mass of substitutions. The observed bands at 521 cm^{-1}, 540 cm^{-1}, 921 cm^{-1} and 596 cm^{-1} in IR spectrum are assigned to the CCC bending mode for the **CET** which are in good agreement with the theoretical values. These assignments are in line with the assignments proposed by the literature [31].

Azo compounds are difficult to identify by IR spectroscopy because no significant bands are observed for them, the azo group being non polar in nature [32-34]. In addition, the weak absorption of azo group occurs in the same region as the absorption of aromatic compounds, the *cis*-form having slightly stronger bands normally than the trans-form. The N=N stretching vibrations are normally occur at 1410-1440 cm^{-1} [35] Crane et al [36]. reported the N-N stretching frequency at 1151 cm^{-1}. In line with above observation N-N stretching is assigned at 1156 cm^{-1} in the present work. The theoretically calculated value by B3LYP/6-311++G(2d,p) at 1162cm^{-1} (mode no. 38) shows that the deviation of about 6cm^{-1}. In the title compound the experimentally observed value of the N=N stretching band (1453 cm^{-1}) shows very good agreement with computed values 1450 cm^{-1} at B3LYP/6-311++G(2d,p) level of theory. The N=N-N-ring in-plane/out-of-plane bending vibrations occurs at 420 and 176 cm^{-1}/360 and 73 cm^{-1} respectively. Due to the heavy mass of the N, the rings themselves are vibrated in (longitudinal) and out (transverse) of the molecular plane and this view is also in line with the above literature.

The N-H stretching vibration is found in this case at 3403 cm^{-1}. The theoretically calculated value by B3LYP/6-311++G(2d,p) at 3374 cm^{-1} (mode no. 1) shows that the deviation of about ~29 cm^{-1} may be due to the presence of intermolecular interactions when compared with experimental observation. This mode is a pure mode as is evident from PED column contributing exactly 100%. Sundaraganesan et al.[37] assigned C–N stretching absorption in the region 1382–1266 cm^{-1} for aromatic amines. In benzamide the band observed at 1368 cm^{-1} is assigned to be due to C–N stretching [38]. In the present work, a strong band at 1207 cm^{-1} in FT-IR has been assigned to C–N stretching vibrations. The C–N stretching vibration is theoretically predicted at 1195 cm^{-1} (mode no. 36) by B3LYP method shows good agreement with experimental observation

The vibrations belonging to the bond between the ring and the halogen atoms are worth to discuss here, since mixing of vibrations are possible due to the lowering of the molecular symmetry and the presence of heavy atoms on the periphery of molecule[39]. The assignments of C–Cl stretching and deformation vibrations have been made by comparison with the halogen-substituted benzene derivatives.[40] Mooney [40-42] assigned vibrations of C–X group (X = Cl, Br, I) in the frequency range of 1129–480cm^{-1}. In FT-IR spectrum of title molecule, a strong band at 1041 cm^{-1} is assigned to C-Cl stretching vibration. The C-Cl bending vibration is assigned to the FT-IR band at 351 and 278 cm^{-1}.

The band observed at 2983 cm^{-1} (mode no. 11) in FT-IR spectrum could be attributed to CH_3 symmetric stretching vibration that shows excellent agreement compared with B3LYP/6-311++G(2d,p) method. There is one methylene group attached to the **CET** molecule. The peaks in the wavenumber range 1476 and 1459 cm^{-1} of **CET** are due to the methylene scissoring modes and are assigned very well at 1468 and 1461 cm^{-1} in the recorded FTIR spectrum. The FT-IR band appearing at 1258cm^{-1} (96% PED) is assigned to methylene twisting mode of vibrations. The methylene rocking mode is calculated at 1135 cm^{-1} with 77% contribution to PED.
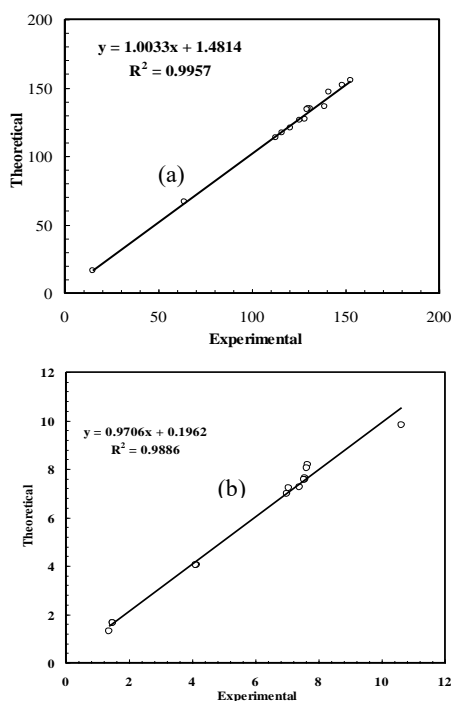
4.3. NMR spectra

^{1}H and ^{13}C NMR chemical shifts were calculated by GIAO method at the level of B3LYP/6-311++G(2d,p). The experimental and theoretical chemical shifts (in ppm relative to TMS) are given in Table 4S. TMS chemical shift calculations were done at the same level of theory as the title molecule. Calculated ^{1}H isotropic chemical shielding for TMS at the B3LYP/6-311++G(2d,p) level was 31.9484 ppm. The ^{13}C isotropic chemical shielding for TMS at this level was 183.454 ppm. Comparing experimental NMR spectra with calculations showed that the theoretical results are in good line with experiments. The correlation coefficient value for ^{1}H NMR is 0.9886 and for ^{13}C NMR is 0.9957 (Fig. 4).
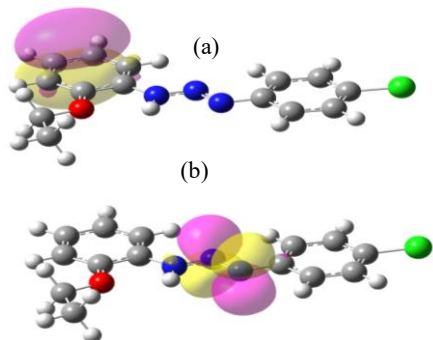
4.4. NBO and AIM analyses

In this paper, we have used NBO and AIM analyses to characterize intra-molecular hydrogen bond. NBO approach quantitatively describes the non-covalent bonding-antibonding interactions (or non-Lewis structure). The interaction values are expressed by means of the second-order perturbation (or delocalization) energy which is shown by E$^{(2)}$.

$\pi \rightarrow \pi^*$ and $n \rightarrow \pi^*$ charge transfers are characterized as conjugative interactions or resonance, $\pi \rightarrow \sigma^*$ and $\sigma \rightarrow \pi^*$ are known as primary hyperconjugation, and $\sigma \rightarrow \sigma^*$ as secondary hyperconjugation [43]. The NBO analysis was done with the level of B3LYP/6-311++G(2d,p). As a default, Gaussian program uses the density of HF method in all post-HF method.
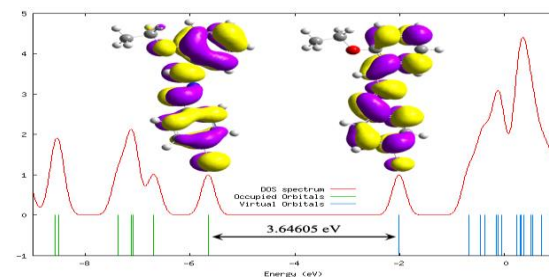
about this conclusion, we have tested the existence of hydrogen bond by atoms in molecules (AIM) theory. Fig. 1c shows the bond critical points that have been calculated by AIM2000 program [14]. The data shows that there is not bond critical point between O···H-N. The absence of intra-molecular hydrogen bond is clear in the experimental data of X-ray crystallography.

Figure 4. Correlation between theoretical and experimental 13C NMR (in DMSO) (a) and 1H NMR (in Acetone) (b) at the level of B3LYP/6-311++G(2d,p) (b).

In order to use the DFT density in this work to analyze the natural bond orbital, the keyword density=current was added in the route section. To visualize the natural bond orbitals, NBOs should be saved in the check point file by the keyword pop=savenbos. The HOMO and LUMO of natural bond orbitals are shown in Fig. 5. This figure shows that the C12-C13 bond is nucleophile and N1=N2 is electrophile.

Table 1. Major donor-acceptor orbital interactions and their second order delocalization energies ($E^{(2)}$) in kcal/mol for the studied compound. All values are in kcal/mol.

Donor→Acceptor	Energy
$\pi_{N1=N2} \rightarrow \pi^*_{C4=C10}$	11.37
$\pi_{C1=C9} \rightarrow \pi^*_{C2=C3}$	18.93
$\pi_{C1=C9} \rightarrow \pi^*_{C4=C10}$	18.34
$\pi_{C2=C3} \rightarrow \pi^*_{C1=C9}$	19.81
$\pi_{C2=C3} \rightarrow \pi^*_{C4=C10}$	18.95
$\pi_{C4=C10} \rightarrow \pi^*_{N1=N2}$	21.48
$\pi_{C4=C10} \rightarrow \pi^*_{C1=C9}$	22.29
$\pi_{C4=C10} \rightarrow \pi^*_{C2=C3}$	19.50
$\pi_{C5=C14} \rightarrow \pi^*_{C6=C11}$	19.71
$\pi_{C5=C14} \rightarrow \pi^*_{C12=C13}$	19.37
$\pi_{C6=C11} \rightarrow \pi^*_{C5=C14}$	17.41
$\pi_{C6=C11} \rightarrow \pi^*_{C12=C13}$	18.92
$\pi_{C12=C13} \rightarrow \pi^*_{C5=C14}$	20.00
$\pi_{C12=C13} \rightarrow \pi^*_{C6=C11}$	19.20
$n_{Cl} \rightarrow \pi^*_{C1=C9}$	12.36
$n_O \rightarrow \pi^*_{C6=C11}$	27.65
$n_{N3} \rightarrow \pi^*_{N1=N2}$	53.41
$n_{N3} \rightarrow \pi^*_{C5=C14}$	36.43
$n_O \rightarrow \sigma^*_{N-H}$	1.07

4.5. HOMO–LUMO energy

In the frontier region, neighboring orbitals are being often closely spaced. In such cases, consideration of only the HOMO and LUMO may not yield a realistic description of the frontier orbitals. For this reason, the density-of-states (DOS) in terms of Mulliken population analysis were calculated using the GaussSum program. The DOS diagram is shown in Fig. 6.

Figure 5. (a) The HOMO ($\pi_{C12=C13}$), and (b) LUMO ($\pi^*_{N1=N2}$) natural bond orbitals for the title molecule.

For a hydrogen bond, there is a high charge transfer (or high second order delocalization) between the lone pair of proton acceptor and anti-bonds of the proton donor. Table 1 shows the second order delocalization energy for some important donor-acceptor orbital interactions. П–electron delocalization in the ring has a range of 17-22 kcal/mole of energy. Results show that the resonance between N=N and ring is less than the in-ring resonance. Table 1 shows that Oxygen conjugate with the ring more than the chlorine. Delocalization energy for $n_O \rightarrow \sigma^*_{N-H}$ is only 1.07 kcal/mol, that shows there is not intra-molecular hydrogen bond within the molecule. To be sure

Figure 6. Partial DOS diagram contain HOMO (left) and LUMO (right) plot of CET at B3LYP/6-311++G(2d,p).

The DOS plot mainly presents the composition of the fragment orbitals contributing to the molecular orbitals. The HOMO–LUMO energy gap of **CET** was calculated at the 6-311++G(2d,p) level, which reveals that the energy gap reflects the chemical activity of the molecule. The LUMO as an electron acceptor represents the ability

to obtain an electron, and HOMO represents the ability to donate an electron. The calculated energies and the energy gap is

LUMO = -2.01065 eV
HOMO = -5.65670 eV
HOMO-LUMO Energy gap = 3.64605 eV

The energy gap (3.64605 eV) of HOMO–LUMO explains the eventual charge transfer interaction within the molecule, which influences the biological activity of the molecule. Consequently, the lowering of the HOMO–LUMO band gap is essentially a consequence of the large stabilization of the LUMO due to the strong electron-acceptor ability of the electron-acceptor group.

5. Conclusions

1-(4-Chlorophenyl)-3-(2-ethoxyphenyl)triazene was synthesized and characterized by elemental analysis, FT-IR, ^{1}H NMR, ^{13}C NMR and X-ray crystallography. The title compound crystallizes in monoclinic system with space group *P2(1)/n*, *a* = 9.3156(3) Å, *b* = 6.1822(2) Å, *c* = 24.5109(8) Å, *α=γ=* 90.00, *β* = 92.678(2)° and *Z* = 4. The molecular structure, IR, ^{1}H NMR, ^{13}C NMR, HOMO-LUMO, NBO and AIM of **CET** are determined and analyzed by theoretical method. Comparisons between the calculated properties the experimental indicate that they support each other and are in good agreement with together.

References

[1] N. C. Monica Barra, I. Lee, N. Chahal, Substituent Effects on the Thermal Cis-to-Trans Isomerization of 1,3-Diphenyltriazenes in Aqueous Solution. *J. Org. Chem.* 67 (2002) 2271-2277.

[2] D. S. Moore, S. D. Robinson, Catenated Nitro genLigands Part II.1 Transition Metal Derivatives of Triazoles, Tetrazoles, Pentazoles, and Hexazine. *Adv. Inorg. Chem.,* 32 (1988) 171-239.

[3] R. Meldola, F. W. Streatfield, LXXII.—Notes on anhydro-bases. I. Ethenyltriamidonaphthalene. *J. Chem. Soc.,* 51 (1887) 691-700.

[4] M. K. Rofouei J. A. Gharamaleki, E. Fereyduni, A. Aghaei, G. Bruno, H. A. Z. Rudbari, Structural and Solution Studies of two Mercury (II) Complexes with [1, 3-Bis (2-ethoxy) benzene] triazene. *Anorg. Allg. Chem.,* 638 (2012) 220-223.

[5] G. A. Casagrande, E. Lang, G. M. de Oliveira, M. Hörner, F. Broch, Dealing with 1,3-bis(4-nitrophenyl)triazene as intermediary ligand in the synthesis of polymeric (μ-Se)Hg-cluters: One-pot synthetic procedures and X-ray structural characterization of [(PhSe)7Hg4BrPy]n. *Inorg. Chim. Acta.,* 360 (2007) 1776-1779.

[6] K. Vrieze, G. Van Koten, Comprehensive Coordination Chemistry, Pergamon Press, Oxford, 1987.

[7] G. M. de Oliveira, M. Hörner, A. Machado, M. A. Villetti, D. F. Back, B. A. Iglesias, Stabilization of substituted triazene oxides by lanthanides chelation: Synthesis, TGA evaluations and X-ray structural features of [MIII{O2NPhNNN(O)Ph}4](Et3NH)·H2O (M = La3+, Dy3+; Et = C2H5). *J. Mol. Struct.,* 928 (2009) 85-88.

[8] Bruker, SAINTPlus. Data Reduction and Correction Program v. 6.01, Bruker AXS, Madison, Wisconsin, USA, 1998.

[9] G. M. Sheldrick, SADABS v.2.01, Bruker/Siemens Area Detector Absorption Correction. Program, Bruker AXS, Madison, Wisconsin, USA, 1998.

[10] G. M. Sheldrick, SHELXTL v. 5.10, Structure Determination Software Suite, BrukerAXS, Madison, Wisconsin, USA, 1998.

[11] Gaussian 03, Revision C.02, M. J. Frisch, G. W. Trucks, H. B. Schlegel, G. E. Scuseria, M. A. Robb, J. R. Cheeseman, J. A. Montgomery, Jr., T. Vreven, K. N. Kudin, J. C. Burant, J. M. Millam, S. S. Iyengar, J. Tomasi, V. Barone, B. Mennucci, M. Cossi, G. Scalmani, N. Rega, G. A. Petersson, H. Nakatsuji, M. Hada, M. Ehara, K. Toyota, R. Fukuda, J. Hasegawa, M. Ishida, T. Nakajima, Y. Honda, O. Kitao, H. Nakai, M. Klene, X. Li, J. E. Knox, H. P. Hratchian, J. B. Cross, V. Bakken, C. Adamo, J. Jaramillo, R. Gomperts, R. E. Stratmann, O. Yazyev, A. J. Austin, R. Cammi, C. Pomelli, J. W. Ochterski, P. Y. Ayala, K. Morokuma, G. A. Voth, P. Salvador, J. J. Dannenberg, V. G. Zakrzewski, S. Dapprich, A. D. Daniels, M. C. Strain, O. Farkas, D. K. Malick, A. D. Rabuck, K. Raghavachari, J. B. Foresman, J. V. Ortiz, Q. Cui, A. G. Baboul, S. Clifford, J. Cioslowski, B. B. Stefanov, G. Liu, A. Liashenko, P. Piskorz, I. Komaromi, R. L. Martin, D. J. Fox, T. Keith, M. A. Al-Laham, C. Y. Peng, A. Nanayakkara, M. Challacombe, P. M. W. Gill, B. Johnson, W. Chen, M. W. Wong, C. Gonzalez, and J. A. Pople, Gaussian, Inc., Wallingford CT, 2004.

[12] NBO Version 3.1, E. D. Glendening, A. E. Reed, J. E. Carpenter, F. Weinhold,

[13] R. F. W. Bader, Atoms in Molecules, A Quantum Theory, Springer, UK, 1990.

[14] F. Biegler-König, J. Schönbohm, D. J. Bayles, AIM2000. *Comput. Chem.,* 22 (2001) 545-559.

[15] M. H. Jamróz, Vibrational Energy Distribution Analysis VEDA 4, Warsaw, 2004.

[16] N. M. O''Boyle, A. L. Tenderholt, K. M. Langner, A Library for Package-Independent Computational Chemistry Algorithms. J. Comp. Chem., 29 (2008) 839-845.

[17] F. H. Allen, O. Kennard, D. G. Watson, L. Brammer, A. G. Orpen, R. Taylor, Tables of bond lengths determined by X-ray and neutron diffraction. Part 1. Bond lengths in organic compounds. *J. Chem. Soc., Perkin Trans.,* 2 (|1987) S1-S19.

[18] A. G. Orpen, L. Brammer, F. H. Allen, O. Kennard, D. G. Watson, R. Taylor, Supplement. Tables of bond lengths determined by X-ray and neutron diffraction. Part 2. Organometallic compounds and co-ordination complexes of the d-and f-block metals *J. Chem. Soc., Dalton Trans.,* 12 (1989) S1-S83.

[19] M. P. Andersson, P. Uvdal, New Scale Factors for Harmonic Vibrational Frequencies Using the B3LYP Density Functional Method with the Triple-ζ Basis Set 6-311+G(d,p). *J. Phys. Chem.* 109 (2005) 2937-2941.

[20] V. K. Rastogi, M. A. Palafox, R. P. Tanwar, L. Mittal, 3,5-Difluorobenzonitrile: ab initio calculations, FTIR and Raman spectra. *Spectrochim. Acta. A.,* 58 (2002) 1987-2004.

[21] M. Silverstein, G. C. Basseler, C. Morill, Spectrometric Identification of Organic Compounds, Wiley, New York, 1981.

[22] G. Keresztury, Raman Spectroscopy: Theory, in: Chalmers, J. M.; Griffiths P. R. (Eds.), Handbook of Vibrational Spectroscopy, Wiley, New York, 2002.

[23] V. Krishnakumar, N. Prabavathi, S. Muthunatesan, Density

functional theory study of vibrational spectra, and assignment of fundamental vibrational modes of 1-bromo 4-fluoronaphthalene. *Spectrochim. Acta. A.,* 70 (2008) 991-996.

[24] M. K. Rofouei, N. Sohrabi, M. Shamsipur; E. Fereyduni, S. Ayyappan, N. Sundaraganesan, X-ray crystallography characterization, vibrational spectroscopy, NMR spectra and quantum chemical DFT/HF study of N,N-di(2-methoxyphenyl)formamidine. *Spectrochim.. Acta. A.,* 76 (2010) 182-190.

[25] E. Fereyduni, M. K. Rofouei, M. Kamaee, S. Ramalingam, S. M. Sharifkhani, Single crystal structure, spectroscopic (FT-IR, FT-Raman, 1H NMR, 13C NMR) studies, physico-chemical properties and theoretical calculations of 1-(4-chlorophenyl)-3-(4-nitrophenyl)triazene. *Spectrochim. Acta. A.* 90 (2012) 193-201.

[26] N. P. G. Roeges, A Guide to the Complete Interpretation of Infrared Spectra of Organic Structures, Wiley, New York, 1994.

[27] G. Varsanyi, Vibrational spectra of benzene derivatives, Akademiai Kiado, Budapest, 1969.

[28] D. N. Sathyanarayana Vibrational spectroscopy theory and application, New Age, New Delhi, 2004.

[29] S. Periandy, S. Mohan, Proceedings National Academic Science, India, 68 (A), III (1998)

[30] V. R. Dani, Organic Spectroscopy, MacGraw Hill, New Delhi, 1995.

[31] H. Abdel-Shafy, H. Perlmutter, H. Kimmel, Vibrational studies of monosubstituted halogenated pyridines. *J. Mol. Struct.,* 42 (1977) 37-49.

[32] L. E. Clougherty, Notes - C=N Stretching Frequency in Infrared Spectra of Aromatic Azomethines. *J. Org. Chem.,* 22 (1957) 462.

[33] R. Kubler, R. W. Luttke, S. Z. Weckherlin, *Electrochem.* 64 (1960) 650.

[34] K. J. Morgan, Infrared spectra and structure of arylazonaphthols. *J. Chem. Soc.,* 20 (1961) 2151-2159.

[35] G. Socrates, Infrared and Raman characteristic group frequencies, Wiley, New York, 2001.

[36] L. G. Crane, D. Wang, L. M. Sears, B. Heynz, K. Carron, *Anal. Chem.* 67 (1995) 360.

[37] N. Sundaraganesan, J. Karpagam, S. Sebastian, J. P. Cornard, *Spectrochimica Acta A* 2009, 73, 11.

[38] R. Shanmugam, D. Sathyanarayana, The spectroscopic (FTIR, FT-IR gas phase and FT-Raman), first order hyperpolarizabilities, NMR analysis of 2,4-dichloroaniline by ab initio HF and density functional methods. *Spectrochim. Acta. A.,* 40 (1984) 11-19.

[39] R. A. Yadav, I. S. Sing, Intermolecular hydrogen-bonding in o-ethyl and m-ethyl phenols. *Ind. J. Pure Appl. Phys.,* 23 (1985) 626-627.

[40] G. Varsanyi, Assignments for Vibrational Spectra of Seven Hundred Benzene Derivatives, Adam Hilger, 1974.

[41] E. F. Mooney, The infra-red spectra of chloro- and bromobenzene derivatives—II. Nitrobenzenes. *Spectrochim. Acta. A.,* 20 (1964) 1021-1032.

[42] E. F. Mooney, The infrared spectra of chloro- and bromobenzene derivatives—I: Anisoles and phenetoles. *Spectrochim. Acta. A.,* 19 (1963) 877-877.

[43] F. Weinhold, C. R. Landis, Valency and bonding, Cambridge University Press, New York, 2005.

How to Cite This Article